The Electrochemical Society
Advancing solid state & electrochemical science & technology

# Analysis of Charge/Discharge Behavior of Lithium-Ion Cells Using Simple and High-Precision Capacity Measurements: Relation between Capacity Degradation Rate and Coulombic Efficiency

View the article online for updates and enhancements.

# Analysis of Charge/Discharge Behavior of Lithium-Ion Cells Using Simple and High-Precision Capacity Measurements: Relation between Capacity Degradation Rate and Coulombic Efficiency

**Atsuko Yamazaki** [z] and **Hajime Miyashiro**

*Central Research Institute of Electric Power Industry (CRIEPI), Yokosuka-shi, Kanagawa 240-0196, Japan*

A simple and high-precision charge/discharge capacity measurement system was constructed by utilizing ordinary apparatuses in order to measure large-capacity (20 Ah class) and long life cells. By using this system, the performance of cells with a practicable charge/discharge rate (C/2) can be measured on several measurement days. This system can obtain the charge/discharge capacity with 5-digit precision (i.e., an error of 10 ppm or less) by averaging the charge/discharge capacity for over 10 cycles, and this precision is required for a useful estimation of battery life during stationary use. A downward cell capacity trend every cycle was quantitatively estimated. Self-discharge, named "reversible loss", which does not affect capacity degradation, was observed. The reversible loss likely results from electrochemical self-discharge process, such as shuttle-like mechanism. A fraction of the reversible loss can be explained by the self-discharge current according to the float charge test.
© 2019 The Electrochemical Society. [DOI: 10.1149/2.0671912jes]

Lithium-ion batteries (LIBs) have recently been applied to electric power storage in Japan because of their high energy efficiency and high energy density. LIBs are expected to provide long-term operation, i.e., over 10 years. To achieve long-term operation, it is important to select suitable LIBs and to understand their degradation properties that depend on the state of charge (SOC), C-rate, rest time and so on. Therefore, it is essential to evaluate battery performance based on charge and discharge conditions. Many research institutions, universities and manufacturers have performed battery evaluations under actual operation conditions, and battery degradation mechanisms have attracted much research interest.

An appropriate method is needed to quickly evaluate the effective lifetime of LIBs. Many lifetime evaluation methods[1–9] have focused on a measurement method for cell capacity by integrating precise measurements of the charge and discharge currents. Measurement of the electric capacity during charging and discharging can be useful for quantitatively estimating the lifetime and degree of degradation of a cell. For assembled batteries of stationary use, precise state of a single cell as a function of time is an important factor for a long-term operation. The state of a single cell can be determined from the capacity retention, coulombic efficiency and capacity degradation rate as a function of time. It is essential to measure these degradation properties of a cell with high accuracy. There are many reports on the relation between CE and degradation.[10–12] In these papers, only Smith et al. referred to not only CE, but also self-discharge by shuttle mechanism.[13] Other than the paper, there is hardly any paper discussing the self-discharge capacity.

Smith et al. proposed the concept of high precision coulometry (HPC), and developed a high-precision charge/discharge system.[9] Moreover, an ultrahigh-precision charger (UHPC) was assembled and used to measure CE with an accuracy of ±0.00003 and precision of ±0.00001.[16] They reported differences in the small-size cell performance with or without electrolyte additives and a surface coating using HPS or UHPC.[9,13–16]

It is known that the relative capacity is expressed as the capacity retention, as shown in Eq. 1.

$$A = R^c \tag{1}$$

where $A$ is the relative capacity, $R$ is the capacity retention and $c$ is the cycle number. Assuming one cycle per day, a 20-year operation corresponds to 7200 cycles. To estimate the relative capacity after 20 years with high accuracy, measurements with 5-digit precision are indispensable.

We constructed a simple and high-precision charge/discharge capacity measurement system by utilizing an ordinary apparatus.

Initially, the obtained precision of the charge/discharge capacity and coulombic efficiency was ±0.00005 for each cycle. Then, the temperature effect was cancelled by averaging the charge/discharge capacity over 10 cycles, and a precision of ±0.00001 was achieved. This system is precise enough to quantitatively analyze the downward capacity trend and the coulombic efficiency.[17]

In this paper, we discuss in detail the charge/discharge capacities obtained using this system. In particular, we focus on the relation between the coulombic efficiency and the capacity degradation rate. We used a large-capacity, 20 Ah class cell, which has been applied for stationary use in Japan, as a test cell.[18,19]

## Experimental

Figure 1 shows a schematic of the measurement system. The charge/discharge voltage and current were obtained by a Keithley 2100/100 (6.5 digits) digital multimeter (DMM). A 50 mΩ shunt resistor (PSB series manufactured by Alfa Electronics) was used for the cycling test. Figure 2 shows the circuit using 10Ω and 1kΩ winding resistors for the float charge test. The circuit for the cycling test can be switched to the circuit used during the float charge test by a remote switch installed outside the thermostatic chamber (SU241 manufactured by ESPEC Corp.). This switch enables a smooth change between the circuits without opening the thermostatic chamber and eliminates any temperature disturbance. The charge/discharge power source was HJ2010 by HOKUTO DENKO Corp.

The 20 Ah class cells (SCiB) were provided by Toshiba Corp. The cells consist of a layered cathode and titanate-based anode.[20] This cell
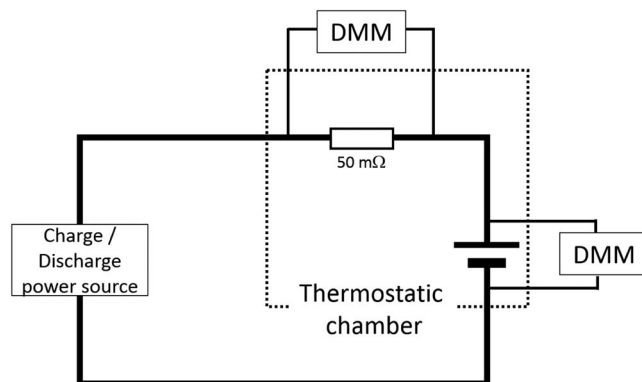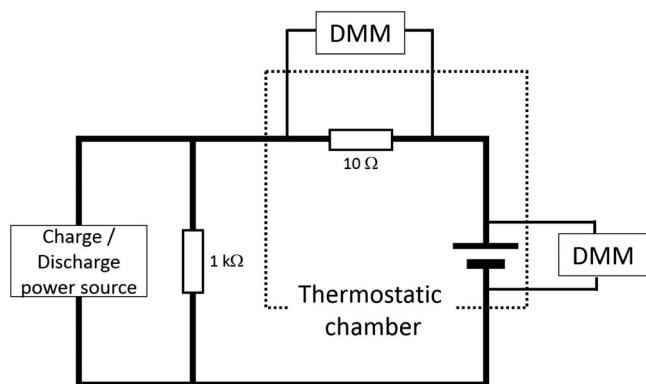


**Figure 1.** Circuit diagram for a simple and high-precision capacity measurement system.

[z]E-mail: y-atsuko@criepi.denken.or.jp

**Figure 2.** Improved circuit diagram for the float test.

is known for its long lifetime. Table I shows the test conditions for cycling operation.

The cells were charged and discharged at a constant current of 10 A (C/2) or 2 A (C/10) between 2.7 and 1.5 V at 45°C or 25°C. The rest time between charge and discharge was 1 or 2 h. The sampling rate of the current and voltage during the cycles was 100 msec.

The float charge current of the cells was measured when the cells were kept at 2.7 V, 2.5 V, 2.3 V, 2.1 V and 1.9 V for over five days. During the float charge test, the test cell was first charged and then held at the target voltage. Then, the test circuit was switched to the float test circuit after the current decreased to less than 100 mA.

## Results and Discussion

To achieve 5-digit precision (i.e., an error of 10 ppm or less), we verified effects of the temperature fluctuation of components such as the shunt resistor, DMM and charge/discharge power source. The examination indicated that the temperature of the shunt resistor and the test cell should remain constant to obtain stable and reliable data. Therefore, we designed a system in which the shunt resistor and the test cell were placed into the thermostatic chamber. According to our simulation results, the required sampling rate was a function of the C-rate applied for stationary use. When cells are charged and discharged for approximately 2 h at C/2-rate operation, there is a possibility of 1 sampling time in the counting error (14 ppm = 1/72000 sampling). This error is prevents 5-digit precision. Thus, the capacities in each cycle were integrated for the region with a stable downward trend, and the integrated capacities from several cycles were averaged to achieve 5-digit precision.

Figure 3 shows the capacity trend and the difference in the coulombic efficiency for C/2 and C/10 rates at 45°C. The capacity linearly decreased as the cycle number increased within the range of the target measurement. A slight fluctuation was ascribed to a temperature fluctuation of ±0.03°C in the thermostatic chamber due to daily variations in the atmosphere. The nominal specification of the thermostatic chamber is ±0.3°C. Upon changing the preset temperature of the thermostatic chamber by one degree, the discharge capacity decreased by approximately 0.035 Ah.[17] This variation is equivalent to an error of 1600 ppm in our experiment. To achieve the target precision of error <10 ppm, the temperature fluctuation must be within ±0.01°C. However, the temperature in the thermostatic chamber cannot be regulated to have less fluctuation, but the temperature fluctuation can be
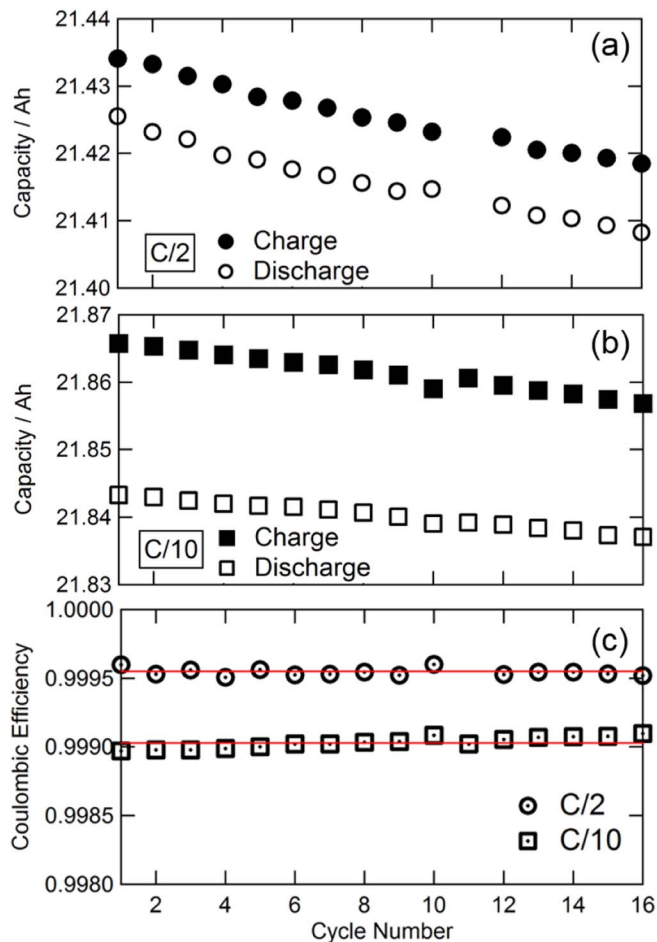


**Figure 3.** Capacity trend and coulombic efficiency at C/2 (a) and C/10 (b) rates at 45°C. The 11th cycle data were not obtained because of communication trouble with the PC.

cancelled by averaging the coulombic efficiency or capacity of each cycle over several days. Finally, a precision of 10 ppm was achieved. The capacities presented in this paper were averaged for more than 10 cycles.

A clear difference between the charge and discharge capacities during cycling was observed. The difference was larger at C/10 than C/2. The slope of the capacity fading, that is, the degradation rate at C/2, was larger than that at C/10. In contrast, the coulombic efficiency at C/2 (0.99955 ± 0.00001) was better than that at C/10 (0.99903 ± 0.00001). A correlation between the coulombic efficiency and the capacity degradation rate was not observed.

Figure 4 shows the magnification of the initial 5 cycles in Fig. 3a. For example, in the third cycle, the charge capacity can be explained by lithium ion transfer from the positive to the negative electrodes. During the subsequent discharge process, lithium ions move from the negative electrode to the positive electrode. However, in the next charge step in the fourth cycle, more lithium ions seem to transfer from the positive electrode to the negative electrode than in the previous discharge process. This phenomenon was observed for the first time by our precise measurement. All electric capacities related to charge/discharge are considered to be comparable to the number of lithium ions moving between the negative and positive electrodes. However, the number of charged and discharged lithium ions is not equal. Figure 3 also shows a decrease in the discharge capacity with cycling. We tried to explain quantitatively the battery capacity by three electric capacity defined as shown in Figure 5. In this figure, the observed electric capacity is the charge/discharge capacity. We defined the coulombic loss as the difference between the charge and discharge capacities in a cycle. The

**Table I. Cycling test conditions.**

| Condition No. | 1 | 2 | 3 | 4 |
|---|---|---|---|---|
| C-rate | C/2 | C/2 | C/10 | C/2 |
| Rest time/h | 1 | 2 | 1 | 1 |
| Temperature/°C | 45 | 45 | 45 | 25 |
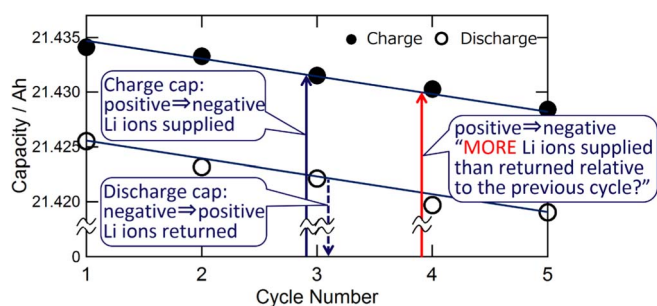
**Figure 4.** Detailed capacity trend of the initial 5 cycles in Figure 3a. Discharge capacity < charge capacity in the subsequent cycle. The difference between the charge and discharge capacity in a cycle is defined as the coulombic loss.
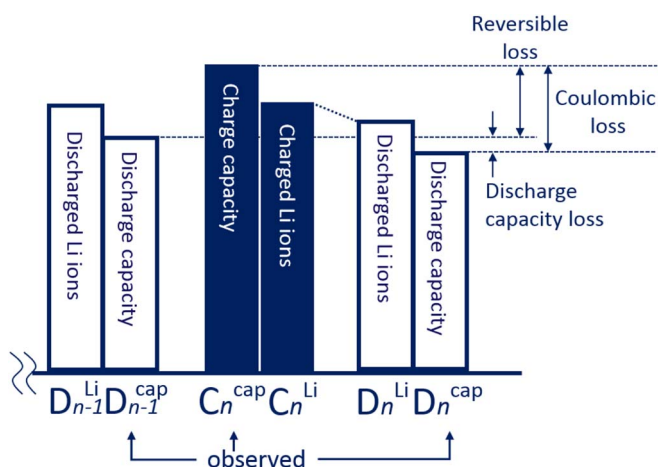


**Figure 5.** The defined coulombic loss, discharge capacity loss and reversible loss. The difference in the discharge capacity between the nth cycle and the n-1th cycle is defined as the discharge capacity loss. The difference between the coulombic loss and the discharge capacity loss is defined as the reversible loss.
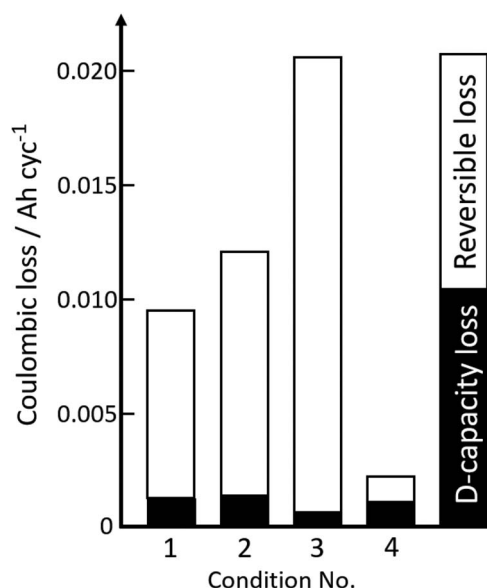


**Figure 6.** Comparison of the coulombic loss under each condition. See Table I for the detailed conditions. Condition 1 shows a standard condition (C/2, 1 h rest, 45°C), 2 shows a rest time change (2 h), 3 shows a C-rate change (C/10), and 4 shows a temperature change (25°C). These condition numbers correspond to Table I.

**Table II. Calculated values of the coulombic loss, discharge capacity loss and reversible loss per cycle with 1 h of rest or 2 h of rest at 45°C.**

|  | Condition 1. | Condition 2. |
|---|---|---|
| C-Rate | C/2 | C/2 |
| Rest time/h | 1 | 2 |
| Temperature/°C | 45 | 45 |
| Coulombic efficiency | 0.99955(1) | 0.99942(1) |
| Coulombic loss/Ah $cyc^{-1}$ | 0.0097(2) | 0.0124(3) |
| Discharge capacity loss/Ah $cyc^{-1}$ | 0.0010(2) | 0.0012(1) |
| Reversible loss/Ah $cyc^{-1}$ | 0.0086(1) | 0.0110(2) |

*The numbers in parentheses are the standard errors for the last digit of the given value. For example, 0.99955(1) means 0.99955 ± 0.00001.

difference in the discharge capacity between a cycle and the previous cycle is defined as the discharge capacity loss. $C_n$ and $D_n$ are denoted as the charge and discharge capacities at the nth cycle, respectively. $C_n^{cap}$ and $D_n^{cap}$ mean charge and discharge electric capacity, respectively. $C_n^{Li}$ and $D_n^{Li}$ indicate the moved lithium amounts at the nth cycle, respectively. Coulombic loss corresponds to $C_n^{cap} - D_n^{cap}$, and coulombic efficiency is $D_n^{cap}/C_n^{cap}$. Discharge capacity loss per cycle corresponds to $D_{n-1}^{cap} - D_n^{cap}$. There is a difference between coulombic loss and discharge capacity loss. The difference is defined as the reversible loss. Table II lists the coulombic loss, discharge capacity loss and reversible loss per cycle with 1 h rest or 2 h rest at 45°C. The discharge capacity loss was similar for the two conditions. On the other hand, the reversible loss was 0.0086 Ah $cyc^{-1}$ and 0.0110 Ah $cyc^{-1}$ for 1 h and 2 h rest, respectively. Reversible loss under 2 h rest conditions was 30% larger than that under 1 h rest conditions. Reversible loss depending on cycle conditions was discussed. Figure 6 indicates the calculated coulombic loss under the conditions in Table II. First, as mentioned above, in a comparison of the Condition 1 and 2, the discharge capacity losses were almost similar. On the other hand, the amount of reversible loss was different. Compared to the Condition 1 and 3, there is a large difference in the coulombic loss. Under the C/10 rate condition, despite the coulombic loss being the largest, the discharge capacity loss was the smallest. A comparison of the Condition 1 and 4 shows a large difference in the coulombic loss. Most of the difference is due to the reversible loss. In this cell system, it was confirmed the discharge capacity loss was smaller than the reversible loss in all cases.

Because the reversible loss does not include the discharge capacity loss, it should not affect the number of active lithium ions residing in the positive and negative electrodes and does not affect the capacities of the electrodes. This phenomenon is considered a self-discharge process as shown in Fig. 7. The self-discharge process in this paper is a rigid discharge that does not affect the capacity degradation. We considered two routes for this self-discharge process. One route may occur thorough electronic conduction inside and/or outside cells, as Process-I in Fig. 7.[21] Another process is an electrochemical shuttle or shuttle-like mechanism inside the cells, as Process-II in Fig. 7.[13,22] Table III shows the apparent resistances assuming that all reversible loss originates from the electronic conduction paths, using the average voltage and the reversible loss in a cycle. The apparent resistance strongly depends on the temperature, and has a lower dependence on

**Table III. Apparent resistance values assuming that all reversible losses originate from electronic conduction paths.**

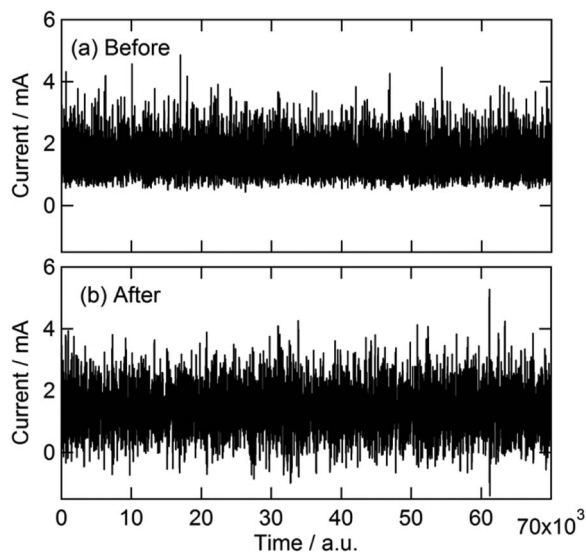| C-rate (Rest time) | 45°C | 25°C |
|---|---|---|
| C/2 (1 h) | 1.7 kΩ | 12.0 kΩ |
| C/2 (2 h) | 1.7 kΩ | 12.0 kΩ |
| C/10 (1 h) | 2.7 kΩ | 12.5 kΩ |
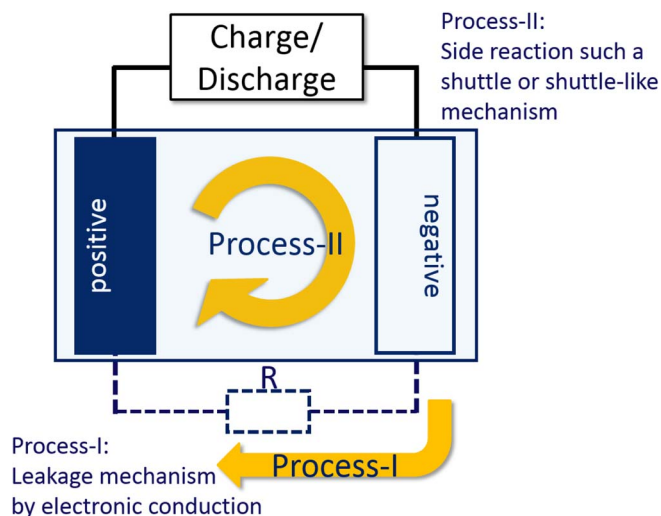
**Figure 7.** The phenomena that are considered to make up reversible loss. Process-I is the electronic conduction leakage mechanism. Process-II is a side reaction such a shuttle mechanism. Process-II is thought to be the main factor causing reversible loss.



**Figure 9.** Histogram of the measurement points corresponding to Fig. 9 (a) before and (b) after the 1 kΩ resistor connection was added.
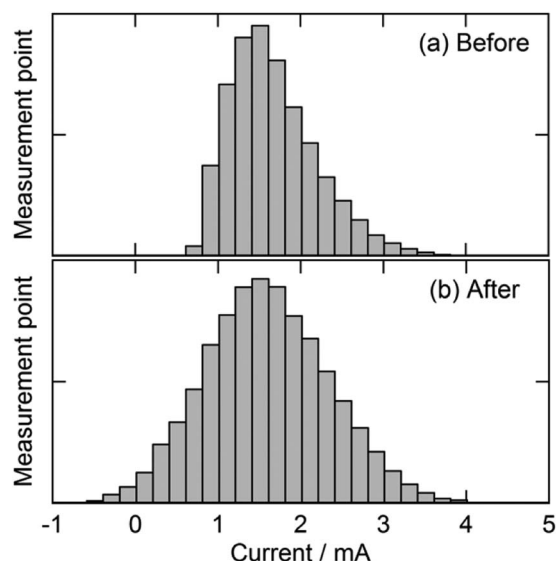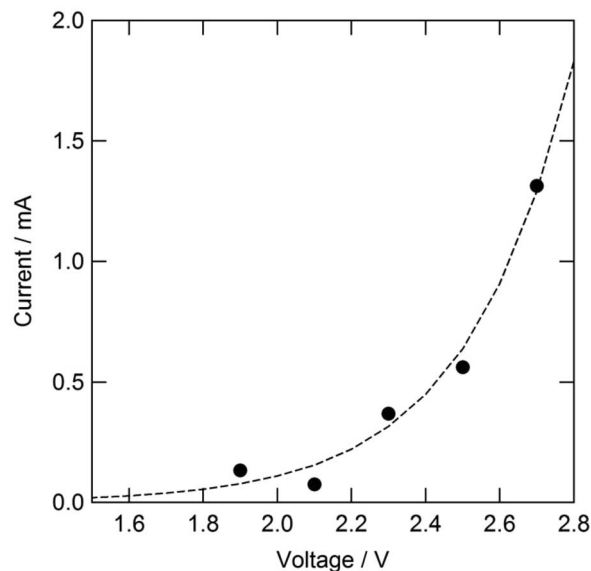
the C-rate. It is difficult to explain the reversible loss considering only the electric conduction. The reversible loss likely results from electrochemical self-discharge processes, such as shuttle-like mechanism.

In order to examine the reversible loss, the leakage current from the cell was measured as a function of the cell voltage. At the time of the first float measurement, an accurate leakage current was not obtained because the cell voltage was higher than the set value caused by thermal or electrical disturbance. Here, a resistor of 1 kΩ was connected in parallel to the cell to drain the extra current, as shown in Fig. 2. Figure 8 shows the float current trend (a) before and (b) after the 1 kΩ resistor was connected once the current reached saturated levels. The current in the float charge test was averaged. Symmetric noise is advantageous for cancelling noise. Figure 9 shows the histograms corresponding to Fig. 8. It is clear that the distribution in Fig. 9b after the 1 kΩ resistor was connected is more symmetric than that in Fig. 9a.

Figure 10 shows the averaged leakage current in the float charge test. The dashed curve is the fitted result. The relationship between

the voltage and the current is nonlinear. Therefore, the self-discharge current is ascribed to the electrochemical process.

Table IV shows the self-discharge capacity, which was estimated from the fitted line in Fig. 10, and the integration of the self-discharge current during the charge, charge-rest and discharge steps in the cycling test. The values for the last raw data show the ratio of the estimated reversible loss over the total amount of integrated self-discharge current during the cycle.

The reversible loss was dynamically measured during charge and discharge. It is difficult to estimate the reversible loss by only statically measuring the steady state current. A fraction of 30 to 40% of the reversible loss can be explained by the self-discharge current because the order of the reversible loss and the self-discharge current is the same. Moreover, the difference of the reversible losses under the quasi-static conditions in the last 1 h of the 2 h rest period was estimated. The reversible losses measured with rest times of 1 h and



**Figure 8.** Float current trend (a) before and (b) after the 1 kΩ resistor connection was added. The measured float current was obtained after taking an average over at least a few days.



**Figure 10.** The self-discharge current values of each tested voltage. The closed circle (•) shows the measurement point, and the dashed line shows the line fitted as y = A exp (B (x-C)).

**Table IV. The calculated self-discharge capacity values for each condition.**

| Condition No. | C-rate (Rest time) | Estimated reversible loss/Ah cyc$^{-1}$ | Measured reversible loss[1]/Ah cyc$^{-1}$ | Ratio[2]/% |
|---|---|---|---|---|
| 1. | C/2 (1 h) | 0.0025 | 0.0086(1) | 29 |
| 2. | C/2 (2 h) | 0.0036 | 0.0110(2) | 33 |
| 3. | C/10 (1 h) | 0.0087 | 0.0208(3) | 42 |
| 4[3] | C/2 (1 h) | - | - | - |

[1]The values of condition No.1 and 2. are identical to those in Table II.
[2]Ratio = (the estimated reversible loss/the measured reversible loss) × 100. The estimated reversible loss means the estimated self-discharge capacity during the charge, charge-rest and discharge steps.
[3]The data were too noisy to calculate the reversible loss.

2 h at the C/2 rate were compared. As a result, approximately 45% of the difference the reversible loss between the 1 h and 2 h rest conditions was explained by the residual current. To further understand the reversible loss, the leakage current mechanism must be elucidated, and enhanced measurement precision is needed for the cycling test.

## Conclusions

We proposed a quantitative analysis method for large-capacity cells using a simple and high-precision charge/discharge capacity measurement system. This measurement system enables measurements to be taken under practical conditions and can measure the charge/discharge capacity with 5-digit precision (i.e., an error of 10 ppm or less) by averaging the integrated capacities of several cycles in a short timeframe. The cell for stationary use evaluated by this system consisted of a layered cathode and titanate-based anode. In this cell system, a correlation between the coulombic efficiency and the capacity degradation rate was not observed.

To quantitatively discuss the obtained data, three concepts, coulombic loss, discharge capacity loss and reversible loss, were defined. In the discharge capacity loss, which is directly associated with the capacity fading of cells, was confirmed to be smaller than the reversible loss in all cases. Moreover, to examine the reversible loss, the leakage current from the cell was measured as a function of the cell voltage. The reversible loss likely results from the electrochemical self-discharge process without cell capacity loss, such as a shuttle or shuttle-like mechanism.

## ORCID

Atsuko Yamazaki https://orcid.org/0000-0002-6440-1861

## References

1. I. Bloom, B. W. Cole, J. J. Sohn, S. A. Jones, E. G. Polzin, V. S. Battaglia, G. L. Henriksen, C. Motloch, R. Richardson, T. Unkelhaeuser, D. Ingersoll, and H. L. Case, *J. Power Sources*, **101**, 238 (2001).
2. P. Ramadass, B. Haran, P. M. Gomadam, R. White, and B. N. Popov, *J.Electrochem.Soc.*, **151**, A196 (2004).
3. T. Yoshida, M. Takahashi, S. Morikawa, C. Ihara, H. Katsukawa, T. Shiratsuchi, and J. Yamaki, *J.Electrochem.Soc.*, **153**, A576 (2006).
4. M. Dubarry, V. Svoboda, R. Hwu, and B. Y. Liaw, *J. Power Sources*, **165**, 566 (2007).
5. E. V. Thomas, I. Bloom, J. P. Christophersen, and V. S. Battaglia, *J. Power Sources*, **184**, 312 (2008).
6. K. Honkura, K. Takahashi, and T. Horiba, *J. Power Sources*, **196**, 10141 (2011).
7. M. B. Pinson and M. Z. Bazant, *J.Electrochem.Soc.*, **160**, A243 (2013).
8. X. Han, M. Ouyang, L. Lu, and J. Li, *Energies*, **7**, 4895 (2014).
9. A. J. Smith, J. C. Burns, S. Trussler, and J. R. Dahn, *J.Electrochem.Soc.*, **157**, A196 (2010).
10. F. Yang, D. Wang, Y. Zhao, K. Tsui, and S. J. Bae, *Energy*, **145**, 486 (2018).
11. J. Wilhelm, S. Seidlmayer, P. Keil, J. Schuster, A. Kriele, R Gilles, and A. Jossen, *J. Power Sources*, **365**, 327 (2017).
12. R. A. Adams, B. Li, J. Kazmi, T. E. Adams, V. Tomar, and V. G. Pol, *Electrochimica Acta*, **292**, 586 (2018).
13. A. J. Smith, J. C. Burns, D. Xiong, and J. R. Dahn, *J.Electrochem.Soc.*, **158**, A1136 (2011).
14. T. M. Bond, J. C. Burns, D. A. Stevens, H. M. Dahn, and J. R. Dahn, *J.Electrochem.Soc.*, **160**, A521 (2013).
15. J. R. Dahn, S. Trussler, S. Dugas, D. J. Coyle, J. J. Dahn, and J. C. Burns, *J.Electrochem.Soc.*, **160**, A251 (2013).
16. J. R. Dahn, J. C. Burns, and D. A. Stevens, *J.Electrochem.Soc. Interface*, Fall **25**(3), 75 (2016).
17. A. Yamazaki, H. Miyashiro, Y. Kobayashi, and Y. Mita, *CRIEPI report*, Q16010 (2017).
18. T. Kobayashi, M. Mizutani, and K. Shimada, *Toshiba review*, **67**(6), (2012).
19. T. Hashimoto, T. Kawamata, and K. Shimada, *Toshiba review*, **70**(9), (2015).
20. N. Takami, H. Inagaki, Y. Tatebayashi, H. Saruwatari, K. Honda, and S. Egusa, *J. Power Sources*, **244**, 469 (2013).
21. M. Park, X. Zhang, M. Chung, G. B. Lees, and A. M. Sastry, *J. Power Sources*, **195**, 7904 (2010).
22. P. Arora, R. E. White, and M. Doyle, *J.Electrochem.Soc.*, **145**(10), 3647 (1998).